Chapter 1

Laser Ablation Applied for Synthesis of Thin Films: Insights into Laser Deposition Methods

Camelia Popescu, Gabriela Dorcioman and
Andrei C. Popescu

Additional information is available at the end of the chapter

http://dx.doi.org/10.5772/65124

Abstract

This chapter will focus on laser ablation applied for thin film deposition. The first thin films deposition method based upon laser ablation was pulsed laser deposition (PLD), that could produce thin films out of metals, ceramics and even temperature resistant organics. The need of depositing increasingly complex and delicate materials, lead to radical modifications of PLD and allowed other laser ablation methods to develop. If complex libraries are to be synthesized two or more plasmas will be mixed and the thin films will have a variable composition over surface. This technique is called Combinatorial PLD (CPLD).

PLD/CPLD are however limited when it comes to organic materials transfer, because the high intensity laser beam can damage them. Matrix Assisted Pulsed Laser Evaporation (MAPLE) is a thin film deposition technique derived from PLD, able to transfer accurately fragile molecules from a target to a substrate, by using a frozen mix made of the material to be deposited and a protective buffer layer.

All these techniques will be discussed in detail with their advantages, drawbacks, influencing factors and applications, while relevant practical examples will be provided in order to make the information easily understandable for the new reader.

Keywords: laser ablation, pulsed laser deposition, matrix-assisted pulsed laser evaporation, thin films, nanoparticles

1. Introduction

A low wavelength of the laser beam and a very short pulse (ns-fs) duration induce instant local vaporization on the surface of a target material generating a plasma plume consisting of photons, electrons, ions, atoms, molecules, clusters, and liquid or solid particles. This phenomenon is known in the literature as '**laser ablation'** [1], a term derived from the Latin word '***ablatio***', meaning 'to carry away'.

Shortly, after the first laser functionality demonstration in 16 May 1960, numerous theoretical and experimental studies were performed concerning the interaction of the high intensity laser beam with solids [2–4], liquids [5], and gases [6].

Laser ablation is the base principle of most applications involving laser processing of materials: precise cutting, hole drilling, laser cleaning of surfaces, compositional analysis, and thin film deposition. The latter came as an obvious application, as a plate/slide/wafer can easily be positioned in front of the plasma plume, acting as a collector for the hot ablated material that condenses in the form of a thin film. This deposition method is known as pulsed laser deposition (PLD). The earliest attempt of thin film deposition was made in 1965 by Smith and Turner [7], but the true breakthrough was achieved by Dijjkamp et al. in 1987 [8], who succeeded the stoichiometric transfer of a compound with a complex molecular structure, very difficult to obtain using other deposition techniques. In this situation, it can be considered that a *congruent ablation* was attained. The decrease in the pulse duration meant laser beams with higher delivered energies that significantly increased the range of materials that could be ablated [9].

Historically, the method was known under several denominations [9]: pulsed laser evaporation, laser induced flash evaporation, laser molecular beam epitaxy, laser assisted deposition and annealing, and laser sputtering.

Some variations in PLD emerged out of necessity to deposit more complex materials or materials degradable at high temperatures. Instead of a single laser beam as in classical PLD, two laser beams can be used simultaneously to ablate two targets mounted on a carousel system, producing a mix of plasmas that will generate thin films with variable composition over the surface. This variation in PLD is known in the literature as combinatorial pulsed laser deposition (CPLD) [10].

Another variation in PLD developed out of necessity to protect compounds with long and fragile molecular chains is called matrix-assisted pulsed laser evaporation (MAPLE), and it uses as the target, a frozen mix consisting of the active material to be deposited and a buffer matrix that preponderantly absorbs the laser beam energy [11].

All these variations in PLD will be discussed in detail in the next chapters with relevant examples for their advantages and drawbacks.

http://dx.doi.org/10.5772/65124

2. Pulsed laser ablation techniques for deposition and compositional analysis

2.1. Pulsed laser deposition (PLD)

The material that is irradiated by the laser beam is called the 'target', while the collector is commonly referred to as the 'substrate'. They have to be placed plan-parallel in a deposition chamber, which is under vacuum conditions. A high intensity laser placed outside the deposition chamber is used as an energy source to ablate the target material and to deposit the thin film. The target vaporization is induced by photons, so no contamination/impurification occurs during the deposition process.

Contrary to this, simplicity of the experimental assembly, the laser-material interaction, which is the PLD base, is a very complex physical phenomenon that involves a succession of different processes [12]. They are:

a. Coupling of the optical energy to the target material.

b. Melting of the surface.

c. Vaporization in form of a plume of the thin upper layer of molten surface.

d. Photon absorption by the vaporized species, which eventually limits the laser fluence at the target surface.

e. Propagation of the plume in the direction normal to the target.

f. Return to the initial state after few nanoseconds from the end of the pulse, with a resolidified surface.

If deposition is made in reactive gas and the obtained film has a composition different from that of the target, the name of the synthesis process is reactive pulsed laser deposition (RPLD). The PLD/RPLD set-up is given in **Figure 1**.

2.1.1. Factors responsible for PLD deposition

Factors influencing the laser ablation process include the following: (i) **deposition conditions** (nature of ambient-ultra-high/high/vacuum, reactive gas, target-substrate separation distance, number of pulses); (ii) **laser beam parameters** (wavelength and pulse duration fluence); and (iii) **material properties of the target** (melting temperature, thermal diffusion rate, optical reflectivity).

Uniform ablation of the target is obtained through its rotation and translation with respect to the laser beam. The distance between the target and substrate is generally of a few centimetres. The film uniformity can be improved if the substrate is moved in the plasma direction, for example, by rotating the substrate holder. The substrate temperature is a very important parameter for the morphology, microstructure, and crystallinity of the deposited films.

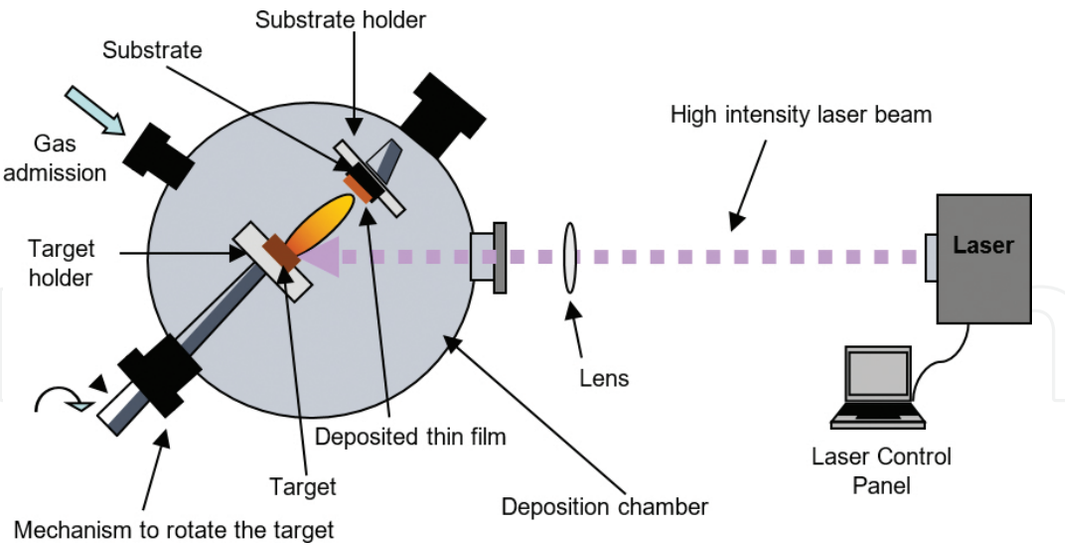

Figure 1. Experimental set-up PLD/RPLD.

2.1.1.1. Deposition conditions

2.1.1.1.1. Influence of the ambient gas inside the deposition chamber

Depending on the structure and composition of the thin films that one desire to achieve by PLD, in the deposition chamber a gas, which can be active or passive, can be introduced. In principle, the passive influence of the gas is necessary because it helps to compensate the eventual losses of the constituent elements. For example, the oxide thin films tend to be oxygen deficient.

We provide a relevant example of ZnO thin films synthesised in a vacuum (4×10^{-2} Pa) and in O_2 (13 Pa) ambient. The aspect of both films was radically different: the films deposited in a vacuum were opaque, dark-coloured (**Figure 2a**), while the films obtained in an oxygen flux were highly transparent (**Figure 2b**) [13].

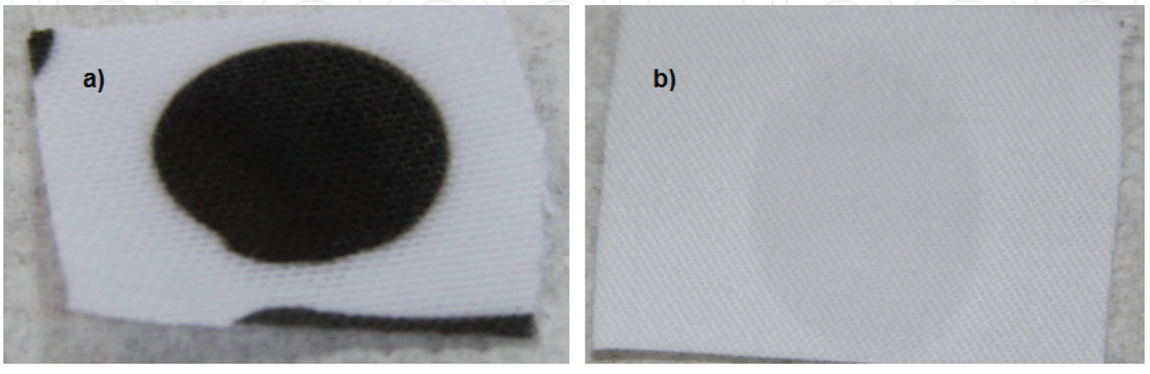

Figure 2. Textile material partially coated with ZnO films: (a) dark-coloured film deposited in vacuum and (b) transparent film deposited in a 13 Pa oxygen flux.

http://dx.doi.org/10.5772/65124

The explanation is that in oxygen ambient, due to the intense collisions with the environmental atoms, the ejected matter is confined to an elongated, 'cigar'- shaped plasma (**Figure 3a**). A thermal equilibrium is reached as a result of collisions during transfer and the substance condenses in large quantities forming compact thin films. In a vacuum, at much lower collision rates, the matter is ejected in all directions (**Figure 3b**), with high energies and speed. These high energetic species are bombarding the layers previously deposited and cause damage (by sputtering off atoms from the outer layers) or defects (dislocations, cracks, holes) on the deposited film. These bombardments occur for each pulse, resulting in a very disordered thin film that is full of defects. The defects are highly absorbent in the visible spectrum and hence the dark aspect.

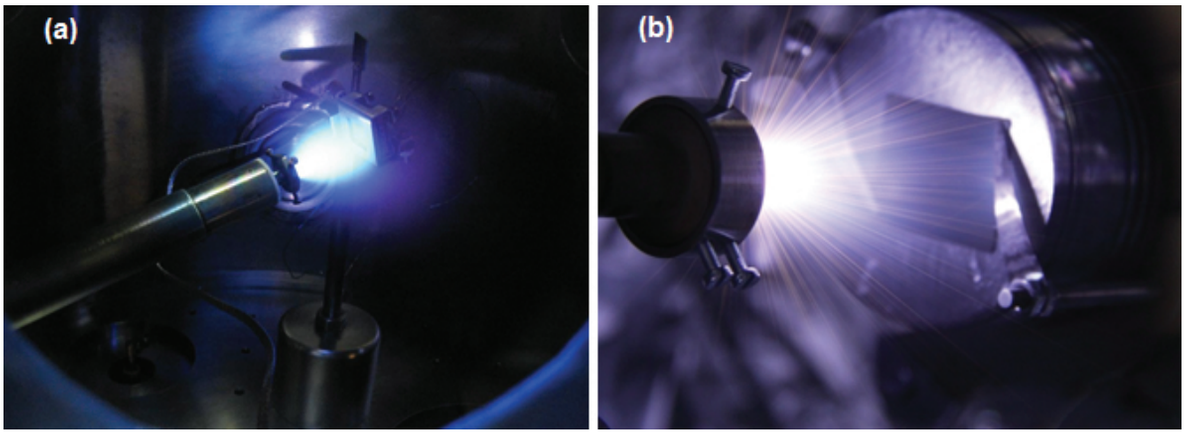

Figure 3. Plasma plume in PLD recorded in 13 Pa O_2 flux (a) and vacuum (b) (Reproduced with permission from Ref. [13]).

2.1.1.1.2. Influence of the target-substrate separation distance

The effect of the target-substrate distance is reflected by the angular scattering of the ejected flux. Different features can occur depending on the position of the substrate. The optimal position of the substrate in order to obtain stoichiometric structures is determined by the plasma evolution. The best depositions (in terms of stoichiometry, uniformity and homogeneity) are obtained when the plasma length is identical with the target-substrate separation distance [13]. To support this assertion we provide an example of ZnO deposition using a low number of pulses and three separation distances: 3, 4, and 5 cm. The plasma plume was 4 cm in length (**Figure 4**).

As shown in **Figure 4**, the largest number of ZnO nanoparticles was present on the surface of the sample placed at 4 cm from the target, while smaller amounts of ZnO nanoparticles were observed for the samples positioned at 3 and 5 cm. As it is known [14], the quantity of deposited substance in PLD is inversely proportional to the square of the target-substrate separation distance. However, this does not apparently apply in our case for the sample placed at 3 cm from the target. A possible explanation could be that the plasma plume deposited and removed

('washed') nanoparticles at the same time from the substrate because the separation distance, in this case, was too small (in any case, smaller than the plasma length).

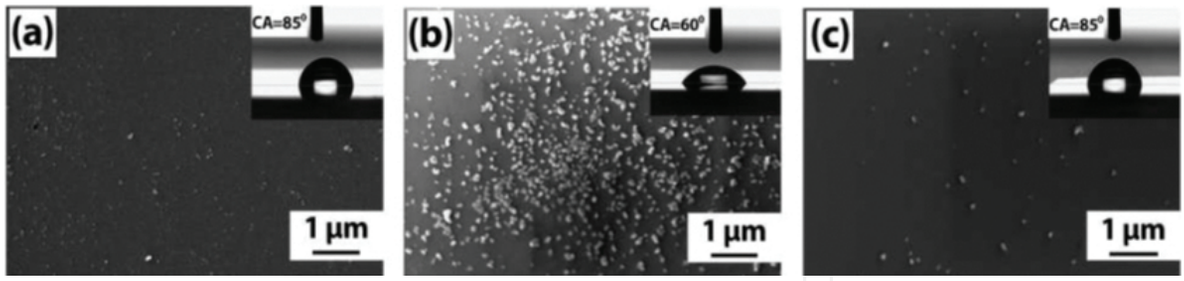

Figure 4. SEM micrographs of ZnO nanoparticles deposited in a 13 Pa O2 flux on a Si substrate. Target-substrate separation distance was of 3 cm (a), 4 cm (b) or 5 cm (c). Inset: water droplet in static mode and the measured CA.

For target-substrate separation distances longer than plasma length, the species in plasma lost their kinetic energy by collisions with other species and gas molecules from the ambient and therefore the ablation rate was significantly lower than for 4 cm.

2.1.1.1.3. Influence of number of pulses

A very low number of pulses (generally under 100) generate a deposition of nano/microparticles on the substrate surface. Slightly increasing the number of pulses produces islands of material. Upon increasing the number of pulses, the substrate is covered by a continuous thin film [15].

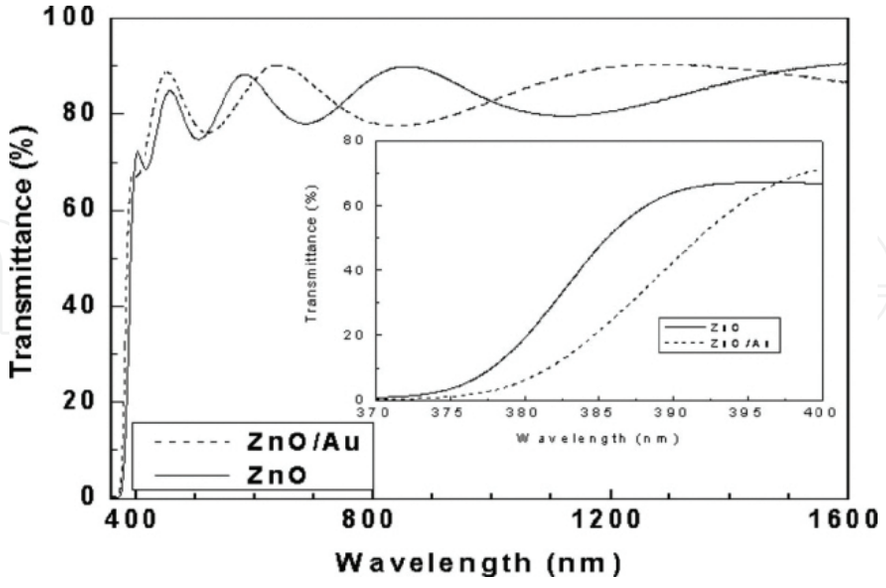

Figure 5. Typical transmission spectra recorded in the case of PLD simple ZnO films (solid curve), and films covered with Au nanoclusters after ablation by 100 pulses from a Au target (dashed curve). (Reproduced with permission from Ref. [15]).

We present a case when ZnO thin films were synthesised by PLD after applying 50,000 pulses to a ZnO target. The target was further switched on with a gold one and by irradiating it with 100 laser pulses Au nanoclusters were generated on the ZnO thin film surface. In **Figure 5**, it can be found that the transmittance spectrum was shifted toward longer wavelengths following the thin film with Au nanoclusters. The infrared band-gap energy was 3.26 eV for ZnO films covered with Au, which is slightly lower than that of simple ZnO films of 3.29 eV [15].

2.1.1.2. Laser beam parameters

2.1.1.2.1. Influence of wavelength and pulse duration

PLD can be applied to vaporize and deposit thin film from any kind of material if the absorbed power density is high enough. The amount of material that is ablated during laser irradiation can be estimated from the thermal diffusion depth, $l_\tau = \sqrt{D \cdot \tau}$, where D is the heat diffusivity in the solid target and τ is the pulse laser duration. The thermal diffusion depth decreases with the duration of the laser pulse.

The delivered laser energy is absorbed by the target material in a layer with thickness given by the formula, $l_s = \frac{1}{\alpha}$, where l_s is known as the optical penetration depth and α is the absorption coefficient for the respective laser wavelength.

The energy delivered by ultra-short laser pulses is absorbed in a thinner layer as compared to ns laser pulses, thus producing higher temperatures at surface level and faster vaporization of the target material [16].

The efficiency of laser beam absorption into the target is closely related to the wavelength that will be used. However, for numerous materials, absorption coefficient dependence on the wavelength can be more complex due to different absorption mechanisms, such as network vibration, free carrier absorption, impurities, and bandgap.

For exemplification, we present the case of Mg film deposition using laser sources with different wavelengths and pulse duration: 308 nm XeCl excimer laser (generating pulses of 30 ns) and 248 nm KrF excimer laser (with 5 ps and 500 fs). Electron microscopy analysis showed that the droplets spread and the density decreased, when using laser pulses with shorter duration [17].

The films deposited using an ns laser source had their surface covered by droplets (**Figure 6a**). These droplets were spherical and had an average diameter of 10 μm. Their presence and morphology are indicative of expulsion of molten material from the surface of the target [18]. In this case, the optical penetration depth $l_s = 2$ μm, (Mg ablated at 308 nm), was less than the thermal diffusion depth, $l_\tau = 17$ μm.

When using ps or fs pulses, the morphology of the Mg film surface changed from droplets covered to smooth surfaces, as shown in **Figure 6b** and **c**. When using ps laser pulses there were still particulates on film surface (not larger than 200 nm) but they completely disappeared

when ablation was conducted with fs pulses. The smoothness of these film surfaces is a consequence of the removal of ablated material with reduced expulsion of melted particles [17].

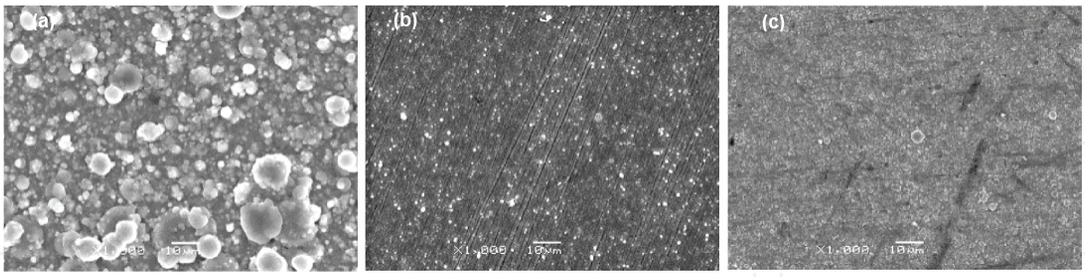

Figure 6. SEM images of Mg thin films deposited by PLD in different regimes: ns (a) ps (b) and fs (c) (Reproduced with permission from Ref. [17]).

2.1.1.2.2. Influence of the laser fluence

The laser pulse fluence can be defined as the optical energy that is delivered to a selected area on the target. Therefore, the fluence can be varied by changing the laser energy or the dimension of the spot area on target.

The coupling of the laser energy to the target surface is dependent on pulse parameters (duration and energy profile), and target characteristics (surface roughness, porosity and density). The fusion and vaporization processes occur only when the laser beam intensity is higher that a *threshold value* defined as the minimal energy of the laser pulse per surface unit that generates plasma ignition.

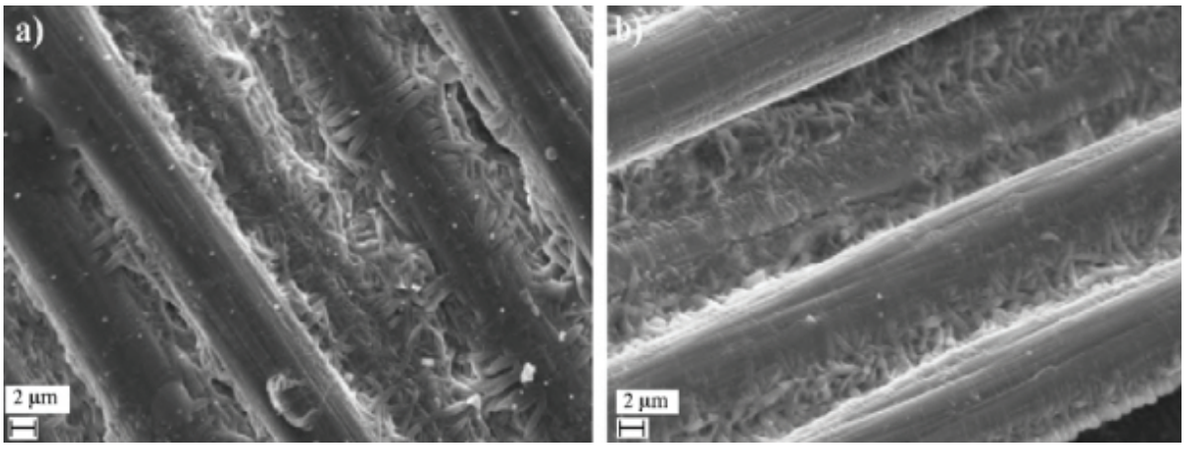

Figure 7. Typical SEM micrographs of TiO_2 nanoparticles deposited on carbon cloth substrate at a laser fluence of 5 (a) and 1 J/cm^2 (b) respectively (Reproduced with permission from Ref. [20]).

For a fixed wavelength and a chosen material, the fluence on the target will have a major effect on the particulate size and density [1]. We present an example where in order to obtain a porous gas diffusion layer, TiO_2 nanoparticles have been deposited at two different laser fluences on carbon

cloth. In the case of 5 J/cm^2 laser fluence, a uniform spatial distribution of nanoparticles over the substrate surface with dimensions of tens to hundreds of nanometres (**Figure 7a** and **b**). Decreasing the laser fluence to 1 J/cm^2 (**Figure 7b**), the number of nanoparticles was considerably reduced and film protuberances were smoother [19].

2.1.2. Advantages of thin film deposition via PLD

1. A major advantage of PLD is related to its large versatility, that is, by control of the deposition parameters, one can obtain thin films with a completely different morphology, structure and/or functionality [20].

We return again to our example of ZnO thin films synthesized by PLD in a vacuum or in oxygen ambient. Just by changing the ambient not only the aspect, but also the wettability behaviour of the films was completely different (**Figure 8**). The thin films were hydrophilic when deposited in an oxygen flux and superhydrophobic (157°) when synthesized in a vacuum. Different conditions changed the Zn and O arrangement in the crystal lattice that influenced the electrical behaviour of the surface [13, 21].

2. The target composition (stoichiometry) can be reproduced with relative ease in the thin films synthesized by PLD. Due to congruent vaporization, it is possible to deposit materials with complex chemical composition. A relevant example is that of hydroxyapatite [$Ca_{10}(PO_4)6(OH)_2$] which is the main constituent of the mineral part of the bone. Thin films of this material have been synthesized by PLD to cover metallic medical implants in view of increasing their bioactivity. EDX analyses revealed the Ca/P ratio of 1.6, very close to the nominal 1.64 value [22, 23].

3. The sequential nature of the PLD process allows for a control of the film thickness through the number of applied pulses.

We provide an example with profiles of TiN films synthesized by PLD by applying to a TiN target 5,000, 10,000 or 20,000 laser pulses [24]. TiN is a hard material, quite difficult to ablate, so the thicknesses of films were quite low, even for a high number of applied pulses. A progressive increase of the TiN films thickness is evidenced in the profiles of **Figure 9**. Films synthesized with 5,000 pulses were of ~60 nm thickness, for 10,000 pulses the thickness was of ~86 nm, while for 20,000, it increased to ~133 nm.

4. Any type of material can be ablated, so the method is not limited to special classes of compounds.

Ceramic, metallic and organic materials have been deposited by PLD. An exhaustive list can be found in the subchapter 2.1.4.

5. Using a carousel system with targets of different compositions, multi-layer films can be obtained. The combinations are endless and new structures with complementary properties can be obtained.

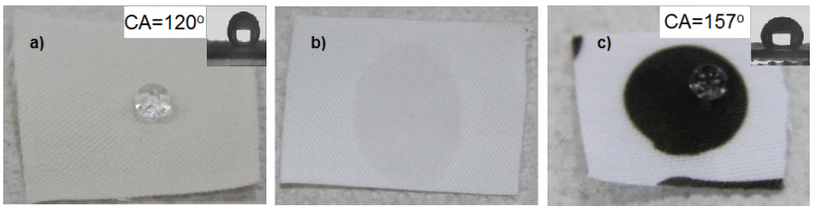

Figure 8. Textile material partially coated with ZnO nanostructures: (a) hydrophobic nanoparticle deposited in vacuum, (b) hydrophilic thin film deposited in 13 Pa oxygen flux, and (c) hydrophobic thin film deposited in vacuum. Inset (a) and (c): water droplet in static mode and the measured CA images were acquired with a EOS 50D digital camera (Canon).

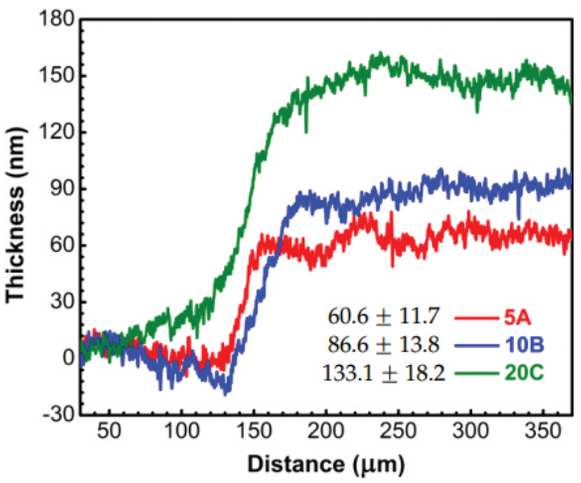

Figure 9. Thickness profiles of TiN layers recorded by profilometry (Reproduced with permission from Ref. [24]).

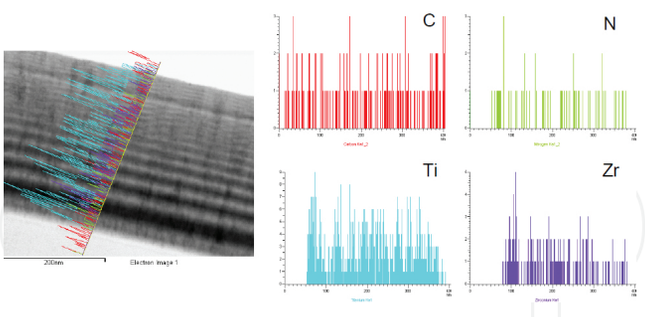

Figure 10. SEM/EDX images recorded for ZrC/TiN multi-layers deposited by PLD (Reproduced with permission from Ref. [26]).

A relevant case of multi-structures ZrC/ZrN and ZrC/TiN is given for exemplification (**Figure 10**). The purpose of this research was to increase the hardness and the elastic modulus of protective coatings. Out of ZrC, ZrN, and TiN single layers, the best results were obtained in case of ZrC with a hardness of 27.6 GPa and a reduced modulus of 228 GPa [25]. For multi-structures, the hardness and reduced modulus increased to similar values between 32.4 and 33.2 GPa and between 251 and 270 GPa, respectively [26].

http://dx.doi.org/10.5772/65124

2.1.3. Drawbacks of PLD

Because the plasma plume is expanding mainly in the *z* direction (see **Figure 11**), the deposition area is usually of a few square centimetres only. Special translation/rotation robotized substrate holders should be used for uniform coating of large substrate areas [9].

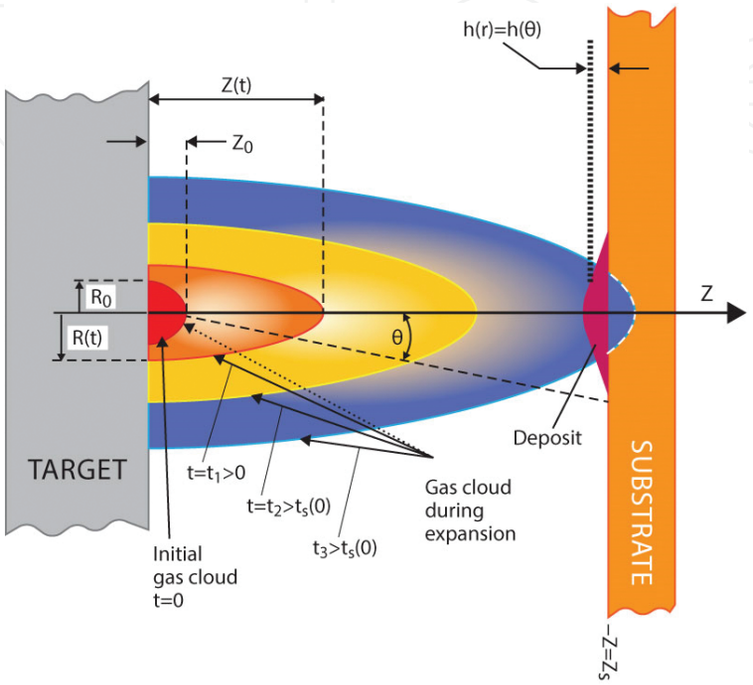

Figure 11. Schematic for the vapor cloud expansion after target irradiation by a laser pulse with energy over the ablation threshold.

Even though PLD deposition of organic materials was reported, generally, this deposition method is not suitable for such compounds—under the action of intense laser pulses, long organic chains can be broken, the deposited material being different from the original target material.

The most important disadvantage however, comes from the micronic and sub-micronic aggregates (known in the literature as particulates or droplets) that hinder applications in fields requiring high finesse (micro or nano-electronics). However, additional procedures in conjunction with PLD can drastically diminish the droplets in PLD films [27–29].

2.1.4. Applications

The idea to use PLD to deposit some of the most varied materials, simple or complex structures with the purpose of obtaining thin films has been rewarded with numerous results published in the literature.

Complex oxide thin films for superconductors ($YBa_2Cu_3O_7$ [30]; $Ba_2Co_2Fe_{12}O_{22}$ [31]), transparent conducting oxides TCO [32–34], active mediums (Er:YAG [35]) wide bandgap electronics (ZnO doped [36]) or in conjunction with other semiconductors [37]), thin films for gas sensors

based on nanostructured tungsten oxide [38, 39], CNx/Si thin heterostructures [40]; complex $(As_2S_3)(100\text{-}x)(AgI)x$ chalcogenide glass [41]; vanadium oxide thin films with various crystal structures [42]; tin oxide for detecting NO_2 [43]; protective coatings and barriers (e.g., DLC [44], BN [45], TiN [46], ZrC [47], ZrN [48, 49], ZrC/TiN and ZrC/ZrN thin multi-layers [50]; TiN biocompatible coatings (prostheses coatings [51–53]); particles for drug delivery [54]; antimicrobial coatings [55]; tissue engineering [56]; organic thin films, i.e., polymethylmetacrylate (PMMA) [57–59]. For biosensor applications: CuO thin film for uric acid biosensor [60], gold-coating of silicon microcantilever for DNA biosensors [61].

2.2. Combinational pulsed laser deposition (CPLD)

One simple approach to study a binary or ternary system is to map all the possible compositions of the phase diagram. Of course, one can synthesize and test one composition at a time, but the disadvantages are the large number of experiments and lots of wasted time. By using a multi-target carousel holder and rhythmically changing the deposition targets during a PLD experiment or two laser beams that irradiate two targets at the same time, one can obtain alternating layers with different periodicities both vertically and horizontally, along the substrate surface (**Figure 12**) [62]. In a single CPLD experiment, thousands of different compositions can be synthesized on a substrate of a few square centimetres [10]. Different stoichiometries can give rise to a variety of different structures and properties. The feasibility and utility of this concept has been demonstrated in the discovery of a number of new materials with much improved physico-chemical properties than the precursors [63–65]. **Figure 12** shows a schematic of a CPLD deposition experiment. The experimental set-up can include two independent laser beams or a split laser beam that hits two targets alternatively or one target at a time, the targets being interchanged with the desired frequency via a mobile carousel.

2.2.1. Advantages of CPLD

1. Thin film libraries can be synthesized in relatively short time (minutes).
2. A large number of new binary or ternary compounds with different properties to study can be obtained.
3. By monitoring the number of laser pulses, one can control the deposition of materials at an atomic layer level. If targets of different nature are used, composite materials will be synthesized.

We give a practical example of IZO (indium-zinc-oxide) compositional libraries synthesized by CPLD [66–69]. Due to the reduced availability of indium, in order to minimize costs, Zn is used for partial replacement of this element. Normally, individual thin films should be synthesized by PLD for measuring their conductivity. By CPLD, we synthesise a library with hundreds of IZO compositions, identify the areas with high conductivity and then we assess the IZO composition using a punctual spectroscopic technique (laser induced breakdown spectroscopy-LIBS). Thus, a significant reduction of time devoted to film deposition and individual analyses could be achieved. LIBS allows fast optical spectra recording and line identification with an excellent spatial resolution (the laser beam is focused at a spot of ≈100

http://dx.doi.org/10.5772/65124

μm diameter), in addition to minimal damage to the film [70, 71]. The quantitative LIBS measurement method, based on the calculation of the spectral radiance of plasma in local thermal equilibrium, was used to measure the Zn/ (In+Zn) ratio and its variation over the length of samples synthesized by CPLD.

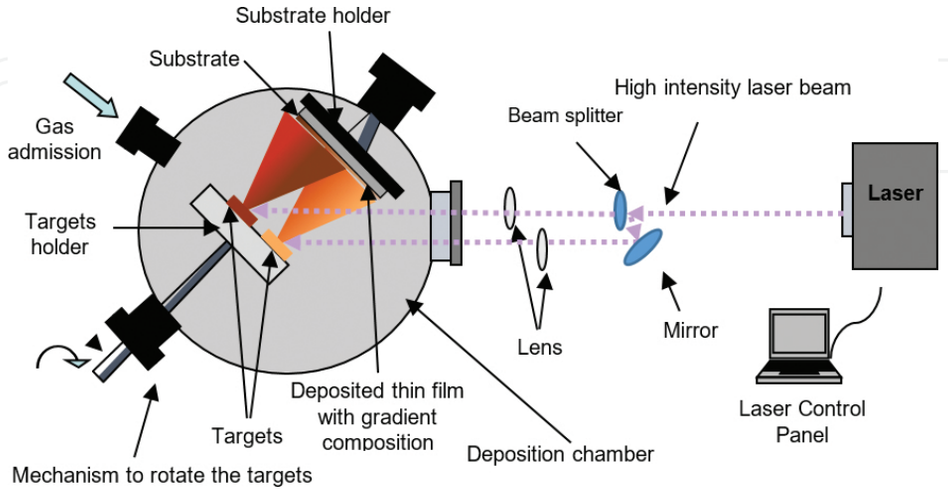

Figure 12. Schematic presentation of a CPLD experiment, along the line the plasmas overlap producing a compositional library.

From the study of the obtained compositional libraries, optimum values of the optical transmittance higher than 85%, resistivity around (5–7) × 10^{-4} Ohm cm and mobility in the (45–53) $cm^2/(V\ s)$ range, were inferred.

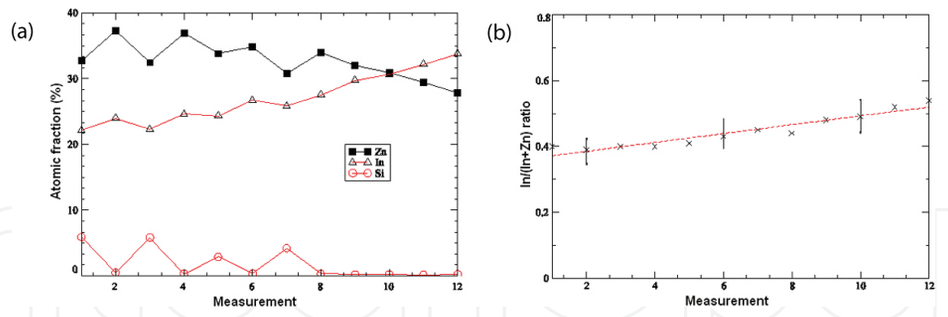

Figure 13. Evolution of (a) In and Zn concentrations and (b) Zn/In ratio on the transversal axis. Twelve measurements were performed on a distance of 6 cm from border towards the centre of the sample (Reproduced with permission from Ref. [72]).

The LIBS measurements started from the border of the glass plate where Zn has the largest concentration, towards the centre of the sample, along the transversal axis [72]. At the border A (close to the ZnO target) the In/(In+Zn) ratio was of 0.40. The trend for this ratio is to increase continuously. Up to measurement 6 (corresponding to 3 cm towards the centre of the sample), it increases by 8%, that is, to a value of 0.44. The Zn decrease and the In increase are almost linear (**Figure 13a**), the overall In/(In + Zn) ratio increases when shifted towards the centre of

the sample. From 3 to 6 cm (in respect with the centre of the sample), the ratio continues its ascendant trend to reach a value of 0.50 at the centre of the film.

In **Figure 13b**, the evolution of the In/(In+Zn) ratio is presented. Starting from the glass border towards the centre, an ascendant trend from 0.40 to 0.54 is observed. Along a distance of 6.5 cm, the In/(In + Zn) ratio increased by 26%. The results are very similar to the values obtained by EDS investigations on the same CPLD samples [73].

2.2.2. Drawback of CPLD

The plasma spread is strongly influenced by the atomic weight of the species. For each type of the target material, new complete compositional tests and mapping should be performed on the resulting films.

2.2.3. Applications

The synthesis of new materials starting from precursors (i.e., BaF_2, SrF_2 and TiO_2 to form (Ba, Sr)TiO_3 [74] or BaF_2 and TiO_2 to form $BaTiO_3$ [75]); deposition of thin film libraries of doped oxide materials: $(Ba_{1-x}Sr_x)TiO_3$ doped with Ca, W, Cr, Mg, Mn, Y and La [74]; libraries of TiO_2 doped with Co [76]; artificial oxide lattices and heterojunctions controlled at an atomic scale [77] ($SrTiO_3$/$BaTiO_3$superlattices); composition spreads: $La_{1-x}Sr_xMnO_3$with $0 \leq x \leq 1$ [78], $Ba_{1-x}Sr_xTiO_3$ [79], $Mg_xZn_{1-x}O$ [80] and IZO [81].

2.3. Matrix-assisted pulsed laser evaporation (MAPLE)

For electronic, optical and biosensor device applications, the materials of choice cover polymeric materials for the fabrication and passivation of electronic coatings, organic dye molecules for non-linear and optical limiting applications, biocompatible and protein coatings for micro-array biosensor applications, and living cells for tissue engineering. The ability to deposit various classes of functional polymeric and organic materials using a single technique provides a significant advantage for their development and implementation.

When a laser interacts with an organic target under the usual conditions for PLD, the material, which is grown in a thin film form, is different from the starting material, the functional groups being often altered [11]. The organic chain can also be broken leaving the film to be made up of smaller polymeric pieces and with different functional groups terminating the ends. Even small changes in the number of functional groups or the degree of polymerization can preclude the use of these films for their desired application. Such modifications might be acceptable for some applications, but in general, the use of lasers for depositing thin films of polymeric and organic materials, requires more subtle approaches than those offered by PLD alone.

MAPLE, a laser based vapour deposition technique derived from PLD, has been developed, at the end of 1990s, to deposit thin organic and biologic films without decomposition or other major irreversible damage [82]. MAPLE is a physical vapour deposition technique capable of depositing uniform thin films over a larger area. Specific to MAPLE is the use of a cryogenic composite target made of a dilute mixture of the polymer/ biopolymer/ protein to be deposited and a light absorbent, and high vapour pressure solvent matrix.

http://dx.doi.org/10.5772/65124

The principal objectives that this technique has to perform are:

a. to avoid the damage of the organic molecules, that can be produced by photochemical and photothermal effects like in the case of PLD;

b. to ensure the deposition of a homogenous thin film, that cannot be obtained by other laser methods.

Changing the target to a frozen composite modifies the laser material interaction, so that the major part of the laser energy is absorbed by the solvent molecules and not by the fragile solute. The rapidly evaporating volatile solvent desorbs the fragile solute by soft collisions and deposits it as a uniform thin film whose properties, such as chemical structure and functionality, have been maintained (**Figure 14**). Since the receiving substrate is kept at room temperature and the sticking coefficient of the solvent is nearly zero, the evaporated solvent is efficiently pumped away by the vacuum system.

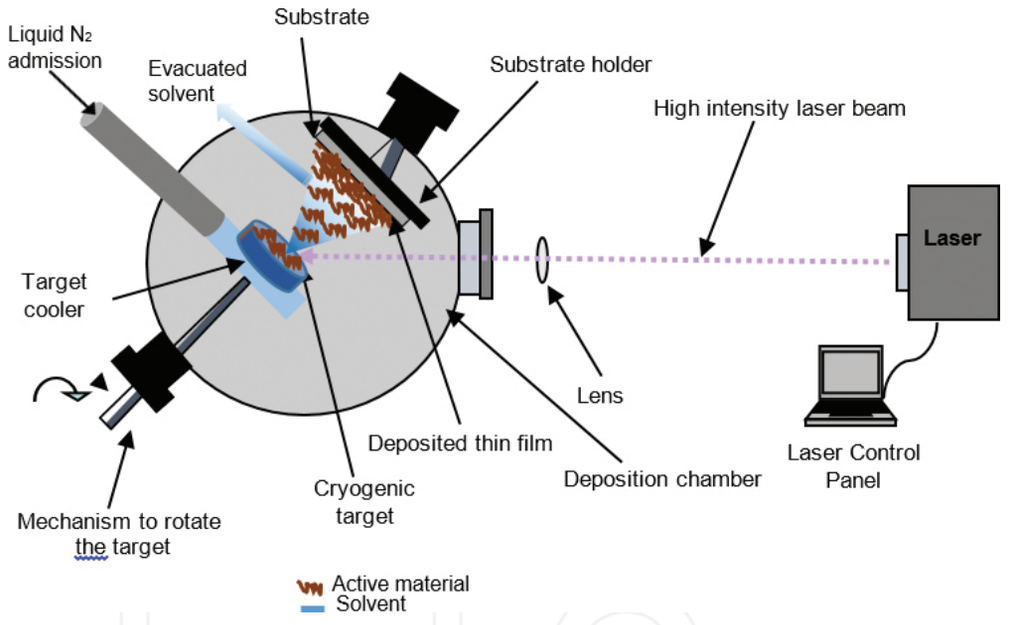

Figure 14. Schematic of material transfer by MAPLE technique.

The MAPLE target is composed of less than 10 wt% of the film material. Each film molecule is surrounded or shielded by a large amount of matrix. This structure prevents the direct thermal and photonic damage to the film material [83].

2.3.1. Factors influencing for MAPLE deposition

The nature of the organic compounds can influence the deposition of a thin film. The laser parameters (fluence, wavelength, and pulse duration) can affect the quality of the thin film.

Although it is derived from PLD, MAPLE differs in certain points, namely the method of preparation of the target and mechanism of laser-material interaction. Film roughness can be

controlled by selecting correctly the appropriate laser fluence, solute concentration and substrate temperature.

2.3.1.1. Influence of the matrix

MAPLE efficiency is determined by the correct choice of the solvent matrix, which has to absorb the laser energy during the deposition, thus protecting the complex organic compound.

The solvent has to satisfy the following conditions:

i. to absorb the laser beam, even when frozen;

ii. to have a high melting point;

iii. to have a high vapour pressure and a high volatility at room temperature, in order to be evacuated very fast from the deposition chamber;

iv. not to be chemically active at laser beam exposure; and

v. to form a uniform solution with the complex organic material.

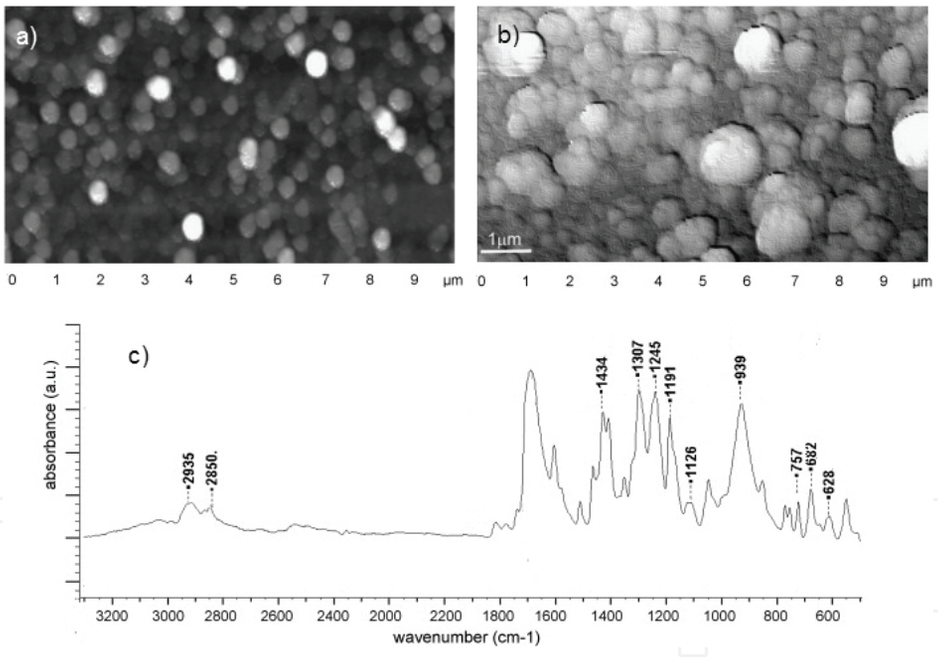

Figure 15. AFM micrographs of P(CPP:SA) 20:80 thin films deposited by MAPLE using ethyl acetate (a) and dimethyl chloride as matrix (b); typical FTIR spectra recorded for P(CPP:SA) 20:80 thin films obtained by MAPLE using ethyl acetate as matrix at a fluence of 0.3 J/cm^2(c). (Reproduced with permission from Ref. [84]).

We present an example of MAPLE thin film synthesis of poly(1,3-bis-(p-carboxyphenoxy, propane)-co-(sebacic anhydride)) (20:80) (P(CPP:SA)20:80) using two different solvents as a matrix to protect this hydrophobic anhydride copolymer [84]. One solvent was dimethyl chloride and the other, ethyl acetate. The copolymer was successfully transferred in both cases, but the morphology of the films was quite different. AFM images presented in **Figure 15a** for

the case of ethyl acetate as the matrix reveal a granular morphology of thin films with individual grains with diameters of ~400 nm. In the case of dimethyl chloride as the matrix, the thin film seems to be compact with some circular (~500 nm in diameter) features splashed on the surface forming a layered plate-like structure (**Figure 15b**). Ethyl acetate was selected as the best solvent based on AFM data and FTIR spectra comparison (**Figure 15c**) that showed a high resemblance between the target material and the thin film.

2.3.1.2. Influence of the laser fluence

McGill and Chrisey [82] proposed in their patent that the laser energy is absorbed majorly by the solvent matrix and is converted in thermic energy producing solvent evaporation. The complex organic compound will reach a kinetic energy high enough that will ensure the transfer and the immobilization onto the substrate.

Georgiou and Kokkinaki [85] advanced the hypothesis that the process takes place due to a photomechanical process (material expulsion). The complex organic compound will be ejected into the gaseous phase only if the laser irradiation takes place at a fluence that surpasses the ablation threshold. When the laser fluence is under the ablation threshold a thermic vaporization process, that produces the solvent desorption, occurs.

Itina et al. [86] suggested that after the laser irradiation upon the organic compound, kinetic energy is a result of both thermic and mechanic phenomena. They proposed a theoretic study that simulates the initial steps of molecule ejection. They observed that when the laser fluence surpasses the ablation threshold, clusters would be ejected from the target. The most important observation was that during the ablation process the organic compound molecules are not fragmented.

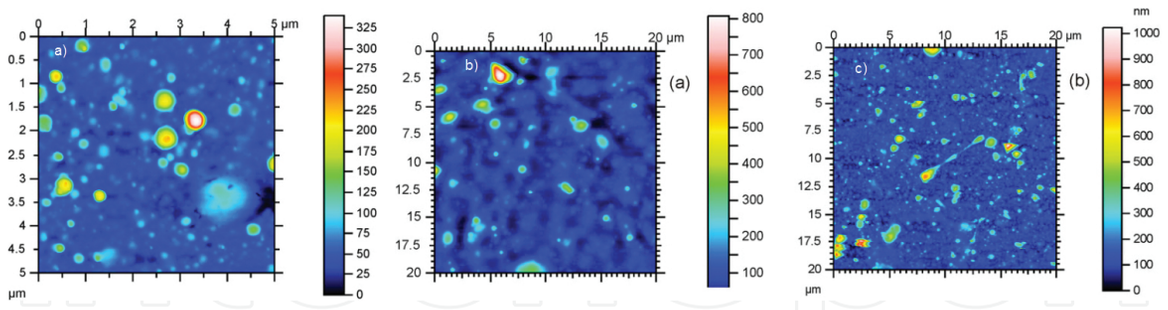

Figure 16. Top view AFM image of the RNase A thin films obtained from a frozen composite target containing 1% (w/v) biomaterial in buffer Hepes solvent, by irradiation with 15,000 subsequent laser pulses at 0.4 (a), 0.5 (b), 0.7 J/cm^2 (c) laser fluence (Reproduced with permission from Ref. [87]).

In their support, we present the example of RNaseA enzyme thin films obtained by MAPLE [87]. When irradiation of targets was conducted with a laser fluence of 0.4 J/cm^2 (**Figure 16a**) the films were constituted of tens of nanometre-sized particles probably generated after surface evaporation and cluster formation in transit towards the substrate. By increasing the laser fluence to 0.5 J/cm^2 (**Figure 16b**), both the mean diameter and the mean height of particles increase and double population could be identified: a majority population of 500 nm mean

diameter and some large micronic particles. At 0.7 J/cm^2 (**Figure 16c**), the film is covered by micrometric particles, caused by the droplet expulsion from the target surface as a result of explosive evaporation or spallation mechanisms [88, 89] termed cold laser ablation [90, 91].

2.3.2. Advantages of material deposition via MAPLE

MAPLE was developed to surmount the difficulties in solvent-based coating technologies such as inhomogeneous films, inaccurate placement of material, and intricate or erroneous thickness control. The process utilizes a low fluence pulsed UV laser and a frozen target consisting of a dilute mixture of the material to be deposited and a high vapour-pressure solvent. The low fluence laser pulse interacts mainly with the volatile solvent, causing its evaporation. During the process, the solute desorbs intact, that is, without any significant decomposition, and is then uniformly deposited on the substrate.

- It enables the thin film deposition from a large amount of organic materials, such as polymers, proteins, enzymes and combination of organic-inorganic materials.

- It is a non-contact deposition technique free of pollution risks for the thin films. The molecular composition and structure of the material that is deposited by MAPLE are preserved during the transfer process.

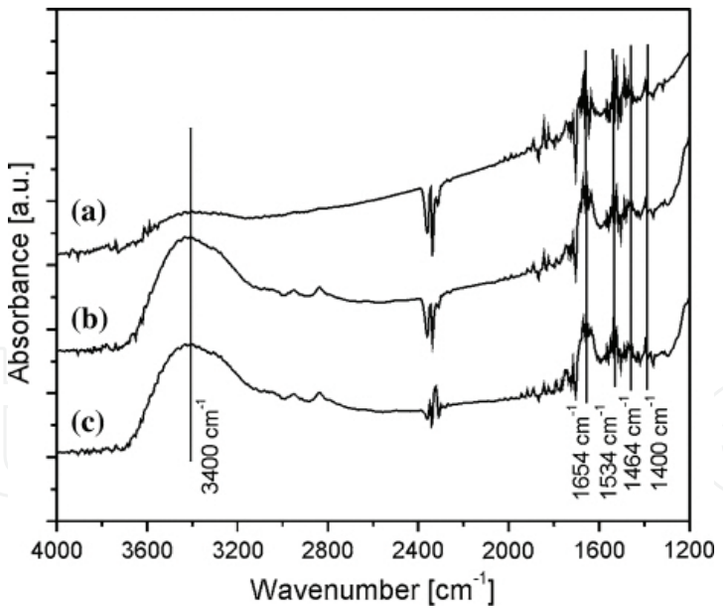

Figure 17. FTIR images of (a) laser immobilized RNase A obtained by the irradiation of 1 wt% frozen composite RNase A target, and the drop-cast samples of (b) initial and (c) final MAPLE target solutions of RNase A in buffer HEPES–NaOH, pH 7.5 (Reproduced with permission from Ref. [92]).

In support of this assertion, we give the FTIR spectra for a RNase A enzyme thin film (**Figure 17a**), for drop-cast of the initial RNase A solution used to prepare MAPLE targets (**Figure 17b**) and for the final RNase A solution, collected from the target holder after the

laser irradiation experiments (**Figure 17c**) [92]. As can be seen in the **Figure 17** the spectrum of the transferred RNase A was comparable to that of the initial drop-cast and to that of the target after irradiation. The bands of RNase A target material were also present in the spectra of deposited films: at 3400 cm^{-1} there was a band characteristic to N–H stretching vibrations from amide I groups; the one at 1654 cm^{-1} corresponded to C=O and C–N stretching vibrations of amide I, while the band at 1464 cm^{-1} was characteristic to in-plane N–H bending as well as C–N stretching vibrations in the same functional group. At 1534 cm^{-1}, the band was associated with tyrosine amino acid residues, while the band at 1400 cm^{-1} could belong to the amide III region [93–95]. The lower band intensity, in case of the MAPLE thin films, was due to the five times lesser amount of RNase A enzyme in the film as compared to the amount present in the drop-cast samples.

2.3.3. Drawbacks of MAPLE

The solvent has to be UV absorbing, therefore the choice is limited and in many cases very difficult.

In order to obtain perfect transfer of the organic material from the target to the substrate, a process optimization procedure is mandatory. Laser beam fluence, repetition rate, and pressure inside the reaction chamber have to be tweaked for each new material to be deposited.

Toxic, volatile solvents are often the only choice for target preparation.

2.3.4. Applications

Biomaterials for drug delivery, antimicrobial systems and biosensors: polyethylene glycol [96–99], polyvinyl alcohol derivatives [100, 101], oligo(*p*-phenylene-ethynylene) [102], magnetite/salicylic acid/silica shell/antibiotics [103], porphyrin [104], laccase [105], urease [106], and lysozyme [107]. Polymers for electronic devices (electrically conductive polymers, light emitting thin films): polythiophene [108], polyfluorene [109], and hybrid composites [110]; CdS quantum dots onto TiO_2 nanotubes for solar cells [111]; Protective coatings: composite carbon/gold nanoparticle films [112].

3. Conclusions

Laser deposition methods have been used to deposit a countless simple or complex inorganic or organic materials. It is quite hard to find other alternative methods that are so easily tunable so that they could produce thin films of so many different materials while preserving in the same time their structure and properties. This is probably the main reason for the endurance of these techniques despite some big outcomes: (i) droplets on film surface, which reduce their use in high tech fields and (ii) small area depositions that prevent their real breakthrough in industry.

Major progress has been achieved to overcome these issues, numerous droplet filters having been proposed in the literature with good results and large scale depositions of up to square metres being reported.

This chapter aimed to show for the new reader just a small part of the myriad of parameters that can be tuned and how important small adjustments can become for the final aspect and the properties of thin films. The combination of various parameters is practically limitless and new structures with interesting properties that emerge from these combinations provide a long life for the research in this field.

The authors hope that after reading this chapter, one will get an idea about the countless applications where laser ablation can be used, for synthesis, tuning or characterization of thin films. It is expected that new methods based on laser ablation will continue to emerge and develop as science progresses and applications become more and more punctual. Laser-patterned deposition of thin films or living cells transfer in a matrix by laser-induced forward transfer, compositional analysis of organic compounds by matrix-assisted laser desorption/ionization are hot emerging fields that rotate around the laser ablation mechanisms.

Acknowledgements

The authors acknowledge financial support from the Romanian National Authority for Scientific Research through the PNII-RU-TE-2012-3-0379 (TE 16/2013) and the National Authority for Research and Innovation in the frame of Nucleus programme under contract 4N/2016.

Author details

Camelia Popescu, Gabriela Dorcioman and Andrei C. Popescu*

*Address all correspondence to: andrei.popescu@inflpr.ro

National Institute for Lasers, Plasma and Radiation Physics, Laser Department, "Laser-Surface-Plasma Interactions" Laboratory, Bucharest-Magurele, Romania

References

[1] Chrisey D.B., Hubler G.K., editors. Pulsed Laser Deposition of Thin Films. 1st ed. New York: Wiley; 1994. 648 p.

[2] Brech F., Cross L. Optical micromission stimulated by a ruby maser. Applied Spectroscopy. 1962;16(2):59

[3] Ready J.F. Development of plume of material vaporized by giant-pulse laser. Applied Physics Letter. 1963;3(1):11–13. DOI: 10.1063/1.1723555

[4] White R.M. Generation of elastic waves by transient surface heating. Journal of Applied Physics. 1963;34(12):3559–3567. DOI: 10.1063/1.1729258

[5] Askar'yan G.A., Prokhorov A.M., Chanturiya G.F., Shilnikov G.P. The effects of a laser beam in a liquid. Journal of Experimental and Theoretical Physics. 1963;17(6):1463–1465.

[6] Meyerand Jr. R.G., Haught, A.F. Gas breakdown at optical frequencies. Physical Review Letters. 1963;11(9):401–403. DOI: 10.1103/PhysRevLett.11.401

[7] Smith H.M., Turner A.F. Vacuum deposited thin films using a ruby laser. Applied Optics. 1965;4(1):147–148. DOI: 10.1364/AO.4.000147

[8] Dijkkamp D., Venkatesan T., Wu X.D., Shaheen S.A., Jisrawi N., Min-Lee Y.H. et al. Preparation of Y-Ba-Cu oxide superconductor thin films using pulsed laser evaporation from high Tc bulk material. Applied Physics Letters. 1987;51(8):619–621. DOI: 10.1063/1.98366

[9] Eason R., editor. Pulsed Laser Deposition of Thin Films: Applications-Lead Growth of Functional Materials. 1st ed. New Jersey: Wiley; 2006.

[10] Koinuma H., Takeuchi I. Combinatorial solid-state chemistry of inorganic materials. Nature Materials. 2004;3(7):429–438. DOI: 10.1038/nmat1157

[11] Chrisey D.B., Pique A., McGill R.A., Horwitz J.S., Ringeisen B.R., Bubb D.M. et al. Laser deposition of polymer and biomaterial films. Chemical Reviews. 2003;103(2):553–576. DOI: 10.1021/cr010428w

[12] Belouet C. Thin film growth by the pulsed laser assisted deposition technique. Applied Surface Science. 1996;96–98(2);630–642. DOI: 10.1016/0169-4332(95)00535-8

[13] Popescu A.C, Duta L., Dorcioman G., Mihailescu I.N., Stan G.E., Pasuk I. et al. Radical modification of the wetting behavior of textiles coated with ZnO thin films and nanoparticles when changing the ambient pressure in the pulsed laser deposition process. Journal of Applied Physics. 2011;110(6): 064321. DOI: 10.1063/1.3639297

[14] Mihailescu I.N., Gyorgy E. Pulsed laser deposition: an Overview. In: Asakura T., editor. International Trends in Optics and Photonics. 4th International Commission for Optics (ICO). Japan: Springer; 1999.

[15] Socol G., Axente E., Ristoscu C., Sima F., Popescu A., Stefan N. et al. Enhanced gas sensing of Au nanocluster-doped or-coated zinc oxide thin films. Journal of Applied Physics. 2007;102(8):083103. DOI: 10.1063/1.2798922

[16] Acquaviva S., Perrone A., Zocco A., Klini A., Fotakis C. Deposition of carbon nitride films by reactive sub-picosecond pulsed laser ablation. Thin Solid Films. 2000;373(1): 266–272. DOI: 10.1016/S0040-6090(00)01095-6

[17] Miglietta P., Cultrera L., Cojanu C., Papadopoulou E.L., Perrone A. Mg-based photocathodes prepared by ns, ps and fs PLD for the production of high brightness electron beams. Applied Surface Science. 2009;255(10):5228–5231. DOI: 10.1016/j.apsusc.2008.07.131

[18] Millon E., Albert O., Loulergue J.C., Etchepare J., Hulin D., Seiler W. et al. Growth of heteroepitaxial ZnO thin films by femtosecond pulsed-laser deposition. Journal of Applied Physics. 2000;88(11):6937–6939. DOI: 10.1063/1.1324679

[19] Dorcioman G., Ebrasu D., Enculescu I., Serban N., Axente E., Sima F. et al. Metal oxide nanoparticles synthesized by pulsed laser ablation for proton exchange membrane fuel cells. Journal of Power Sources. 2010;195(23):7776–7780. DOI: 10.1016/j.jpowsour.2009.09.060

[20] Papadopoulou E.L., Zorba V., Pagkozidis A., Barberoglou M., Stratakis E., Fotakis C. Reversible wettability of ZnO nanostructured thin films prepared by pulsed laser deposition. Thin Solid Films. 2009;518(4):1276–1270. DOI: 10.1016/j.tsf.2009.02.077.

[21] Duta L., Popescu A.C., Dorcioman G., Mihailescu I.N., Stan G., Zgura I. et al. ZnO thin films deposited on textile material substrates for biomedical applications. In: Vaseashta A., Braman E., Susmann P., editors. Technological Innovations in Sensing and Detection of Chemical, Biological, Radiological, Nuclear Threats and Ecological Terrorism. NATO Science for Peace and Security Series A: Chemistry and Biology ed. Netherlands: Springer; 2012

[22] Mihailescu N., Stan G.E., Duta L., Chifiriuc M.C., Bleotu C., Sopronyi M. et al. Structural, compositional, mechanical characterization and biological assessment of bovine-derived hydroxyapatite coatings reinforced with MgF_2 or MgO for implants functionalization. Materials Science and Engineering: C. 2016;59:863–874. DOI: 10.1016/j.msec.2015.10.078

[23] Eraković S., Janković A., Ristoscu C., Duta L., Serban N., Visan A. et al. Antifungal activity of Ag: hydroxyapatite thin films synthesized by pulsed laser deposition on Ti and Ti modified by TiO_2 nanotubes substrates. Applied Surface Science. 2014;293:37–45. DOI: 10.1016/j.apsusc.2013.12.029

[24] Duta L., Stan G.E., Popa A.C., Husanu M.A., Moga S., Socol M., et al. Thickness Influence on in vitro biocompatibility of titanium nitride thin films synthesized by pulsed laser deposition. Materials. 2016;9(1):38. DOI: 10.3390/ma9010038

[25] Craciun D., Socol G., Dorcioman G., Stefan N., Bourne G., Craciun V. High quality ZrC, ZrC/ZrN and ZrC/TiN thin films grown by pulsed laser deposition. Journal of Optoelectronics and Advanced Materials. 2010;12(3):461–465.

[26] Craciun D., Bourne G., Socol G., Stefan N., Dorcioman G., Lambers E. et al. Characteristics of ZrC/ZrN and ZrC/TiN multilayers grown by pulsed laser deposition. Applied Surface Science. 2011;257(12):5332–5336. DOI: 10.1016/j.apsusc.2010.11.106

[27] Yoshitake T., Nagayama K.. The velocity distribution of droplets ejected from Fe and Si targets by pulsed laser ablation in a vacuum and their elimination using a vane-type velocity filter. Vacuum. 2004;74(3–4):515–520. DOI: 10.1016/j.vacuum.2004.01.051

[28] Yoshitake T., Shiraishi G., Nagayama K.. Elimination of droplets using a vane velocity filter for pulsed laser ablation of $FeSi_2$. Applied Surface Science. 2002;197–198:379–383. DOI: 10.1016/S0169-4332(02)00344-6

[29] György E., Mihailescu I.N., Kompitsas M., Giannoudakos A. Deposition of particulate-free thin films by two synchronised laser sources: effects of ambient gas pressure and laser fluence. Thin Solid Films. 2004;446(2):178–183. DOI: 10.1016/j.tsf.2003.09.071

[30] Develos-Bagarinao K., Yamasaki H., Nakagawa Y., Endo, K. Relationship between composition and surface morphology in YBCO films deposited by large-area PLD. Physica C: Superconductivity. 2004;412–414(2):1286–1290. DOI: 10.1016/j.physc.2004.01.172

[31] Sudakar C., Subbanna G.N., Kutty T.R.N. Hexaferrite–FeCo nanocomposite particles and their electrical and magnetic properties at high frequencies. Journal of Applied Physics. 2003;94(9):6030–6033. DOI: 10.1063/1.1614848

[32] Gondoni P., Ghidelli M., Di Fonzo F., Bassi A.L., Casari C.S. Fabrication of nano-engineered transparent conducting oxides by pulsed laser deposition. Journal of Visualized Experiments. 2013;72:50297. DOI: 10.3791/50297

[33] Cho H., Douglas E.A., Gila B.P., Craciun V., Lambers E.S., Ren F. et al. Band offsets in HfO_2/$InGaZnO_4$ heterojunctions. Applied Physics Letters. 2012;100(1):012105. DOI: 10.1063/1.3673905

[34] Douglas E.A., Scheurmann A., Davies R.P., Gila B.P., Cho H., Craciun V. et al. Measurement of SiO_2/$InZnGaO_4$ heterojunction band offsets by X-ray photoelectron spectroscopy. Applied Physics Letters. 2011;98(24):242110. DOI: 10.1063/1.3600340

[35] Stanoi D., Popescu A., Ghica C., Socol G., Axente E., Ristoscu C. et al. Nanocrystalline Er: YAG thin films prepared by pulsed laser deposition: an electron microscopy study. Applied Surface Science. 2007;253(19):8268–8272. DOI: 10.1016/j.apsusc.2007.02.113

[36] Ohtomo A., Kawasaki M., Sakurai Y., Ohkubo I., Shiroki R., Yoshida Y. et al. Fabrication of alloys and superlattices based on ZnO towards ultraviolet laser. Materials Science and Engineering: B. 1998;56(2–3):263–266. DOI: 10.1016/S0921-5107(98)00218-9

[37] Ohta H., Hirano M., Nakahara K., Maruta H., Tanabe T., Kamiya M. et al. Fabrication and photoresponse of a pn-heterojunction diode composed of transparent oxide semiconductors, p-NiO and n-ZnO. Applied Physics Letters. 2003;83(5):1029–1031. DOI: 10.1063/1.1598624

[38] Palla-Papavlu A., Filipescu M., Schneider C.W., Antohe S., Ossi P.M., Radnoczi G. et al. Direct laser deposition of nanostructured tungsten oxide for sensing applications.

Journal of Physics D Applied Physics. 2016;49(20):205101. DOI: 10.1088/0022-3727/49/20/205101

[39] György E., Socol G., Mihailescu I.N., Ducu C., Ciuca, S. Structural and optical characterization of WO3 thin films for gas sensor applications. Journal of Applied Physics. 2005;97(9):093527. DOI: 10.1063/1.1889246

[40] Simeonov S., Szekeres A., Gyorgy E., Mihailescu I.N, A. Perrone A. CNx/Si thin heterostructures for miniaturized temperature sensors. Journal of Applied Physics. 2004;95(9):5111–5115. DOI: dx.doi.org/10.1063/1.1691482

[41] Kolev K., Popov C., Petkova T., Petkov P., Mihailescu I.N., Reithmaier J.P. Complex (As2S3)(100−x)(AgI)x chalcogenide glasses for gas sensors. Sensors and Actuators B: Chemical. 2009;143(1):395–399. DOI: 10.1016/j.snb.2009.08.016

[42] Huotari J., Lappalainen J., Puustinen J., Spetz A.L. Gas sensing properties of pulsed laser deposited vanadium oxide thin films with various crystal structures. Sensors and Actuators B: Chemical. 2013;187:386–394. DOI: 10.1016/j.snb.2012.12.067

[43] Starke T.K., Coles G.S., Ferkel H. High sensitivity NO2 sensors for environmental monitoring produced using laser ablated nanocrystalline metal oxides. Sensors and Actuators B: Chemical. 2002;85(3):239–245. DOI: 0.1016/S0925-4005(02)00114-4

[44] Mosaner P., Bonelli M., Miotello A. Pulsed laser deposition of diamond-like carbon films: reducing internal stress by thermal annealing. Applied Surface Science. 2003;208–209:561–565. DOI: 10.1016/S0169-4332(02)01383-1

[45] Marotta V., Orlando S., Parisi G.P., Santagata A. Boron nitride thin films deposited by RF plasma reactive pulsed laser ablation. Applied Surface Science. 2003;208:575–581. DOI: 10.1016/S0169-4332(02)01386-7

[46] Pelletier H., Carradò A., Faerber J., Mihailescu I.N. Microstructure and mechanical characteristics of hydroxyapatite coatings on Ti/TiN/Si substrates synthesized by pulsed laser deposition. Applied Physics A. 2011;102(3):629–640. DOI: 10.1007/s00339-010-6144-8

[47] Craciun D., Socol G., Stefan N., Mihailescu I.N., Bourne G., Craciun V. High-repetition rate pulsed laser deposition of ZrC thin films. Surface and Coatings Technology. 2009;203(8):1055–1058. DOI: 10.1016/j.surfcoat.2008.09.039

[48] Craciun D., Socol G., Dorcioman G., Simeone D., Gosset D., Behdad S. et al. Ar ions irradiation effects in ZrN thin films grown by pulsed laser deposition. Applied Surface Science. 2015;336:129–132. DOI: 10.1016/j.apsusc.2014.10.032

[49] Dorcioman G., Socol G., Craciun D., Argibay N., Lambers E., Hanna M. et al. Wear tests of ZrC and ZrN thin films grown by pulsed laser deposition. Applied Surface Science. 2014;306:33–36. DOI: 10.1016/j.apsusc.2013.12.048

[50] Craciun D., Socol G., Dorcioman G., Niculaie S., Bourne G., Zhang J. et al. Wear resistance of ZrC/TiN and ZrC/ZrN thin multilayers grown by pulsed laser deposition. Applied Physics A. 2013;110(3):717–722. DOI: 10.1007/s00339-012-7224-8

[51] Nelea V., Pelletier H., Iliescu M., Werckmann J., Craciun V., Mihailescu I.N. et al. Calcium phosphate thin film processing by pulsed laser deposition and in situ assisted ultraviolet pulsed laser deposition. Journal of Materials Science: Materials in Medicine. 2002;13(12):1167–1173. DOI: 10.1023/A:1021150207350

[52] Angelina J.T., Ganesan S., Panicker T.M., Narayani R., Paul Korath M., Jagadeesan K. Pulsed laser deposition of silver nanoparticles on prosthetic heart valve material to prevent bacterial infection. Materials Technology: Advanced Performance Materials. 2016. Forthcoming. DOI: 10.1080/10667857.2016.1160503

[53] Rajesh P., Mohan N., Yokogawa Y., Varma H. Pulsed laser deposition of hydroxyapatite on nanostructured titanium towards drug eluting implants. Materials Science and Engineering: C. 2013;33(5):2899–2904. DOI: 10.1016/j.msec.2013.03.013

[54] Singh R.K., Kim W.S., Ollinger M., Craciun V., Coowantwong I., Hochhaus G. et al. Laser based synthesis of nanofunctionalized particulates for pulmonary based controlled drug delivery applications. Applied Surface Science. 2002;197–198:610–614. DOI: 10.1016/S0169-4332(02)00408-7

[55] Gittard S.D., Narayan R.J., Jin C., Ovsianikov A., Chichkov B.N., Monteiro-Riviere N.A. et al. Pulsed laser deposition of antimicrobial silver coating on Ormocer® microneedles. Biofabrication. 2009;1(4):041001. DOI: 10.1088/1758-5082/1/4/041001

[56] Kuppuswamy H., Ganesan A. Structural, mechanical and in vitro studies on pulsed laser deposition of hydroxyapatite on additive manufactured polyamide substrate. International Journal of Bioprinting. 2016;2(2):85–94. DOI: 10.18063/IJB.2016.02.008

[57] Cristescu R., Socol G., Mihailescu I.N., Popescu M, Sava F., Ion E. et al. New results in pulsed laser deposition of poly-methyl-methacrylate thin films. Applied Surface Science. 2003;208–209:645–650. DOI: 10.1016/S0169-4332(02)01415-0

[58] Wang L.D., Kwok H.S. Pulsed laser deposition of organic thin films. Thin Solid Films. 2000;363(1–2):58–60. DOI: 10.1016/S0040-6090(99)00983-9

[59] Kecskemeti G., Smausz T., Kresz N., Toth Z., Hopp B., Chrisey D. et al. Pulsed laser deposition of polyhydroxybutyrate biodegradable polymer thin films using ArF excimer laser. Applied Surface Science. 2006;253(3):1185–1189. DOI: 10.1016/j.apsusc.2006.01.084

[60] Jindal K., Arora K., Tomar M., Gupta V.Uric acid biosensor based on pulsed laser deposited CuO thin film. Journal of Nanoscience Letters. 2012;2:28

[61] Rebollar E., Sanz M., Esteves C., Martínez N.F., Ahumada Ó., Castillejo M. Gold coating of micromechanical DNA biosensors by pulsed laser deposition. Journal of Applied Physics. 2012;112(8): 084330. DOI: 10.1063/1.4761986

[62] Craciun D., Socol G., Stefan N., Miroiu M., Mihailescu I.N., Galca A.C. et al. Structural investigations of ITO-ZnO films grown by the combinatorial pulsed laser deposition technique. Applied Surface Science. 2009;255(10):5288–5291. DOI: 10.1016/j.apsusc.2008.07.120

[63] Xiang X.D., Sun X., Briceno G., Lou Y. A combinatorial approach to materials discovery. Science. 1995;268(5218):1738–1740. DOI: 10.1126/science.268.5218.1738

[64] Briceno G., Chang H., Sun X., Schultz P.G., Xiang X.D. A class of cobalt oxide magnetoresistance materials discovered with combinatorial synthesis. Science. 1995;270(5234):273–275. DOI: 10.1126/science.270.5234.273

[65] Danielson E., Devenney M., Giaquinta D.M., Golden J.H., Haushalter R.C., McFarland E.W. et al. A rare-earth phosphor containing one-dimensional chains identified through combinatorial methods. Science. 1998;279(5352):837–839. DOI: 10.1126/science.279.5352.837

[66] Minami T. Substitution of transparent conducting oxide thin films for indium tin oxide transparent electrode applications. Thin Solid Films. 2008;516(7):1314–1321. DOI: 10.1016/j.tsf.2007.03.082

[67] Hanak J.J. A quantum leap in the development of new materials and devices. Applied Surface Science. 2004;223(1):1–8. DOI: 10.1016/S0169-4332(03)00902-4

[68] Bassim N.D., Schenck P.K., Otani M., Oguchi H. Model, prediction, and experimental verification of composition and thickness in continuous spread thin film combinatorial libraries grown by pulsed laser deposition. Review of Scientific Instruments. 2007;78(7):072203. DOI: 10.1063/1.2755783

[69] Widjonarko N.E., Perkins J.D., Leisch J.E., Parilla P.A., Curtis C.J., Ginley D.S. et al. Stoichiometric analysis of compositionally graded combinatorial amorphous thin film oxides using laser-induced breakdown spectroscopy. Review of Scientific Instruments. 2010;81(7):073103. DOI: 10.1063/1.3455218

[70] Cristoforetti G., De Giacomo A., Dell'Aglio M., Legnaioli S., Tognoni E., Palleschi V. et al. Local thermodynamic equilibrium in laser-induced breakdown spectroscopy: beyond the McWhirter criterion. Spectrochimica Acta Part B: Atomic Spectroscopy. 2010;65(1):86–95. DOI: 10.1016/j.sab.2009.11.005

[71] Aragón C., Aguilera J.A. Characterization of laser induced plasmas by optical emission spectroscopy: a review of experiments and methods. Spectrochimica Acta Part B: Atomic Spectroscopy. 2008;63(9):893–916. DOI: 10.1016/j.sab.2008.05.010

[72] Popescu A.C., Beldjilali S., Socol G., Craciun V., Mihailescu I.N., Hermann J. Analysis of indium zinc oxide thin films by laser-induced breakdown spectroscopy. Journal of Applied Physics. 2011;110(8):083116. DOI: 10.1063/1.3656448

[73] Socol G., Galca A.C., Luculescu C.R., Stanculescu A., Socol M., Stefan N. et al. Tailoring of optical, compositional and electrical properties of the $In_xZn_{1-x}O$ thin films obtained

by combinatorial pulsed laser deposition. Digest Journal of Nanomaterials and Biostructures. 2011;6(1):107–115.

[74] Chang H., Gao C., Takeuchi I., Yoo Y., Wang J., Schultz P.G. et al. Combinatorial synthesis and high throughput evaluation of ferroelectric/dielectric thin-film libraries for microwave applications. Applied Physics Letters. 1998;72(17):2185–2187. DOI: 10.1063/1.121316

[75] Takeuchi I., Chang K., Sharma R.P., Bendersky L.A., Chang H., Xiang X.D. et al. Microstructural properties of (Ba, Sr) TiO_3 films fabricated from $BaF_2/SrF_2/TiO_2$ amorphous multilayers using the combinatorial precursor method. Journal of Applied Physics. 2001;90(5):2474–2478. DOI: 10.1063/1.1388563

[76] Matsumoto Y., Takahashi R., Murakami M., Koida T., Fan X.J., Hasegawa T. et al. Ferromagnetism in Co-doped TiO_2 rutile thin films grown by laser molecular beam epitaxy. Japanese Journal of Applied Physics. 2001;40(11B):L1204–1206. DOI: 10.1143/JJAP.40.L1204

[77] Ohnishi T., Komiyama D., Koida T., Ohashi S., Stauter C., Koinuma H. et al. Parallel integration and characterization of nanoscaled epitaxial lattices by concurrent molecular layer epitaxy and diffractometry. Applied Physics Letters. 2001;79(4):536–538. DOI: 10.1063/1.1385587

[78] Fukumura T., Ohtani M., Kawasaki M., Okimoto Y., Kageyama T., Koida T. et al. Rapid construction of a phase diagram of doped Mott insulators with a composition-spread approach. Applied Physics Letters. 2000;77(21):3426–3428. DOI: 10.1063/1.1326847

[79] Chang K.S., Aronova M., Famodu O., Takeuchi I., Lofland S.E., Hattrick-Simpers J.R. et al. Multimode quantitative scanning microwave microscopy of in situ grown epitaxial $Ba_{1-x}Sr_xTiO_3$ Composition Spreads. Applied Physics Letters. 2001;79(26):4411–4413. DOI: 10.1063/1.1427438

[80] Takeuchi I., Yang W., Chang K.S., Aronova M.A., Venkatesan T., Vispute R.D. et al. Monolithic multichannel ultraviolet detector arrays and continuous phase evolution in $Mg_xZn_{1-x}O$ composition spreads. Journal of Applied Physics. 2003;94(11):7336–7340. DOI: 10.1063/1.1623923

[81] Taylor M.P., Readey D.W., Teplin C.W., van Hest M.F., Alleman J.L., Dabney M.S. et al. The electrical, optical and structural properties of $In_xZn_{1-x}O_y$ ($0 \circledcirc x \circledcirc 1$) thin films by combinatorial techniques. Measurement Science and Technology. 2004;16(1):90–94. DOI: 10.1088/0957-0233/16/1/012

[82] Mc Gill R.A., Chrisey D.B. Method of producing a film coating by matrix assisted pulsed laser deposition. US Patent 6025036. 2000.

[83] Piqué A., Auyeung R.C., Stepnowski J.L., Weir D.W., Arnold C.B., McGill R.A. et al. Laser processing of polymer thin films for chemical sensor applications. Surface and Coatings Technology. 2003;163–164:293–299. DOI: 10.1016/S0257-8972(02)00606-0

[84] Cristescu R., Cojanu C., Popescu A., Grigorescu S., Nastase C., Nastase F. et al. Processing of poly (1, 3-bis-(p-carboxyphenoxy propane)-co-(sebacic anhydride)) 20: 80 (P (CPP: SA) 20: 80) by matrix-assisted pulsed laser evaporation for drug delivery systems. Applied Surface Science. 2007;254(4):1160–1173. DOI: 10.1016/j.apsusc.2007.09.029

[85] Kokkinaki O., Georgiou S. Laser ablation of cryogenic films: implications to matrix-assisted pulsed laser deposition of biopolymers and dedicated applications in nanotechnology. Digest Journal of Nanomaterials and Biostructures. 2007;2(2):221–241.

[86] Itina T.E., Zhigilei L.V., Garrison B.J. Matrix-assisted pulsed laser evaporation of polymeric materials: a molecular dynamics study. Nuclear Instruments and Methods in Physics Research Section B: Beam Interactions with Materials and Atoms. 2001;180(1–4):238–244. DOI: 10.1016/S0168-583X(01)00423-2

[87] Popescu C., Roqueta J., Del Pino A.P., Moussaoui M., Nogués M.V., György E. Processing and immobilization of enzyme Ribonuclease A through laser irradiation. Journal of Materials Research. 2011;26(06):815–821. DOI: 10.1557/jmr.2010.55

[88] Dingus R.S., Scammon R.J. Grüneisen-stress-induced ablation of biological tissue. InOptics, Electro-Optics, and Laser Applications in Science and Engineering. In: Laser-Tissue Interaction II; January 20, 1991; Los Angeles. Proc. SPIE 1427; 1991. DOI: 10.1117/12.44088

[89] Cramer R., Haglund Jr. R.F., Hillenkamp F.. Matrix-assisted laser desorption and ionization in the O─H and C═O absorption bands of aliphatic and aromatic matrices: dependence on laser wavelength and temporal beam profile. International Journal of Mass Spectrometry and Ion Processes. 1997;169–170:51–67. DOI: 10.1016/S0168-1176(97)00223-1

[90] Leveugle E., Ivanov D.S., Zhigilei L.V. Photomechanical spallation of molecular and metal targets: molecular dynamics study. Applied Physics A. 2004;79(7):1643–1655. DOI: 10.1007/s00339-004-2682-2

[91] Mercado A.L., Allmond C.E., Hoekstra J.G., Fitz-Gerald J.M. Pulsed laser deposition vs. matrix assisted pulsed laser evaporation for growth of biodegradable polymer thin films. Applied Physics A. 2005;81(3):591–599. DOI: 10.1007/s00339-004-2994-2

[92] Popescu C., Popescu A.C., Iordache I., Motoc M., Pojoga D., Simon-Gruita A. et al . Structure and enzymatic activity of laser immobilized ribonuclease A. Journal of Materials Science. 2014;49(12):4371–4378. DOI: 10.1007/s10853-014-8136-0

[93] Neault J.F., Diamantoglou S., Beauregard M., Nafisi S., Tajmir-Riahi H.A. Protein unfolding in drug-RNase complexes. Journal of Biomolecular Structure and Dynamics. 2008;25(4):387–394. DOI: 10.1080/07391102.2008.10507187

[94] Georg H, Wharton CW, Siebert F. Temperature induced protein unfolding and folding of RNase A studied by time-resolved infrared spectroscopy. Laser Chemistry. 1999;19(1–4):233–235. DOI: 10.1155/1999/28202

[95] Kong J., Yu S. Fourier transform infrared spectroscopic analysis of protein secondary structures. Acta Biochimica et Biophysica Sinica. 2007;39(8):549–559. DOI: 10.1111/j.1745-7270.2007.00320.x

[96] Califano V., Bloisi F., Vicari L.R., Colombi P., Bontempi E., Depero L.E . MAPLE deposition of biomaterial multilayers. Applied Surface Science. 2008;254(22):7143–7148. DOI: 10.1016/j.apsusc.2008.05.295

[97] Cristescu R., Popescu C., Popescu A., Grigorescu S., Mihailescu I.N., Mihaiescu D. et al. Functional polyethylene glycol derivatives nanostructured thin films synthesized by matrix-assisted pulsed laser evaporation. Applied Surface Science. 2009;255(24):9873–9876. DOI: 10.1016/j.apsusc.2009.04.110

[98] Cristescu R., Popescu C., Popescu A.C., Grigorescu S., Duta L., Mihailescu I.N. et al. Laser processing of polyethylene glycol derivative and block copolymer thin films. Applied Surface Science. 2009;255(10):5605–5610. DOI: 10.1016/j.apsusc.2008.09.060

[99] Paun I.A., Moldovan A., Luculescu C.R., Dinescu M. Antibacterial polymeric coatings grown by matrix assisted pulsed laser evaporation. Applied Physics A. 2013;110(4):895–902. DOI: 10.1007/s00339-012-7193-y

[100] Grumezescu V., Holban A.M., Iordache F., Socol G., Mogoşanu G.D., Grumezescu A.M. et al. MAPLE fabricated magnetite@eugenol and (3-hidroxybutyric acid-co-3-hidroxyvaleric acid)–polyvinyl alcohol microspheres coated surfaces with anti-microbial properties. Applied Surface Science. 2014;306:16–22. DOI: 10.1016/j.apsusc.2014.01.126

[101] Cristescu R., Popescu C., Popescu A.C., Grigorescu S., Duta L., Mihailescu I.N. et al. Functionalized polyvinyl alcohol derivatives thin films for controlled drug release and targeting systems: MAPLE deposition and morphological, chemical and in vitro characterization. Applied Surface Science. 2009;255(10):5600–5604. DOI: 10.1016/j.apsusc.2014.01.126

[102] Ge W., Yu Q., López G.P., Stiff-Roberts A.D . Antimicrobial oligo (p-phenyleneethynylene) film deposited by resonant infrared matrix-assisted pulsed laser evaporation. Colloids and Surfaces B: Biointerfaces. 2014;116:786–792. DOI: 10.1016/j.colsurfb.2014.01.033

[103] Mihaiescu D.E., Cristescu R., Dorcioman G., Popescu C.E., Nita C., Socol G. et al. Functionalized magnetite silica thin films fabricated by MAPLE with antibiofilm properties. Biofabrication. 2012;5(1):015007. DOI: 10.1088/1758-5082/5/1/015007

[104] Iordache S., Cristescu R., Popescu A.C., Popescu C.E., Dorcioman G., Mihailescu I.N. et al. Functionalized porphyrin conjugate thin films deposited by matrix assisted pulsed laser evaporation. Applied Surface Science. 2013;278:207–210. DOI: 10.1016/j.apsusc.2013.01.080

[105] Verrastro M., Cicco N., Crispo F., Morone A., Dinescu M., Dumitru M. et al. Amperometric biosensor based on Laccase immobilized onto a screen-printed electrode by

Matrix Assisted Pulsed Laser Evaporation. Talanta. 2016;154:438–445. DOI: 10.1016/j.talanta.2016.03.072

[106] György E., Sima F., Mihailescu I.N., Smausz T., Hopp B., Predoi D. et al. Biomolecular urease thin films grown by laser techniques for blood diagnostic applications. Materials Science and Engineering: C. 2010;30(4):537–541. DOI: 10.1016/j.msec.2010.02.003

[107] Purice A., Schou J., Kingshott P., Dinescu M. Production of active lysozyme films by matrix assisted pulsed laser evaporation at 355 nm. Chemical Physics Letters. 2007;435(4–6):350–353. DOI: 10.1016/j.cplett.2006.12.078

[108] Bloisi F., Cassinese A., Papa R., Vicari L., Califano V. Matrix-assisted pulsed laser evaporation of polythiophene films. Thin Solid Films. 2008;516(7):1594–1598. DOI: 10.1016/j.tsf.2007.03.159

[109] Tunno T., Caricato A.P., Caruso M.E., Luches A., Martino M., Romano F. et al. Matrix-assisted pulsed laser evaporation of polyfluorene thin films. Applied Surface Science. 2007;253(15):6461–6464. DOI: 10.1016/j.apsusc.2007.01.024

[110] Pate R., Lantz K.R., Stiff-Roberts A.D. Resonant infrared matrix-assisted pulsed laser evaporation of CdSe colloidal quantum dot/poly [2-methoxy-5-(2′-ethylhexyloxy)-1, 4-(1-cyano vinylene) phenylene] hybrid nanocomposite thin films. Thin Solid Films. 2009;517(24):6798–6802. DOI: 10.1016/j.tsf.2009.06.018

[111] Bjelajac A., Petrovic R., Socol G., Mihailescu I.N., Enculescu M., Grumezescu V. et al. CdS quantum dots sensitized TiO_2 nanotubes by matrix assisted pulsed laser evaporation method. Ceramics International. 2016;42(7):9011–9017. DOI: 10.1016/j.ceramint.2016.02.159

[112] Hunter C.N., Check M.H., Bultman J.E., Voevodin A.A. Development of matrix-assisted pulsed laser evaporation (MAPLE) for deposition of disperse films of carbon nanoparticles and gold/nanoparticle composite films. Surface and Coatings Technology. 2008;203(3):300–306. DOI: 10.1016/j.surfcoat.2008.09.003